Budget Analysis of Escherichia coli at a Southern Lake Michigan Beach

ARTICLE *in* ENVIRONMENTAL SCIENCE AND TECHNOLOGY · FEBRUARY 2010

Impact Factor: 5.33 · DOI: 10.1021/es902232a · Source: PubMed

6 AUTHORS, INCLUDING:

Pramod Thupaki
Fisheries and Oceans Canada
7 PUBLICATIONS **53** CITATIONS
SEE PROFILE

David J. Schwab
University of Michigan
132 PUBLICATIONS **2,483** CITATIONS
SEE PROFILE

Meredith Becker Nevers
United States Geological Survey
53 PUBLICATIONS **1,525** CITATIONS
SEE PROFILE

Environ. Sci. Technol. **2010,** *44,* 1010–1016

Budget Analysis of *Escherichia coli* at a Southern Lake Michigan Beach

PRAMOD THUPAKI,[†] MANTHA S. PHANIKUMAR,*[,†] DMITRY BELETSKY,[‡] DAVID J. SCHWAB,[§] MEREDITH B. NEVERS,[||] AND RICHARD L. WHITMAN[||]

Department of Civil & Environmental Engineering, Michigan State University, East Lansing, Michigan, CILER, School of Natural Resources and the Environment, University of Michigan, Ann Arbor, Michigan, NOAA Great Lakes Environmental Research Laboratory (GLERL), Ann Arbor, Michigan, and Lake Michigan Ecological Research Station, U.S. Geological Survey, Porter, Indiana

Received July 24, 2009. Revised manuscript received November 6, 2009. Accepted December 1, 2009.

Escherichia coli (EC) concentrations at two beaches impacted by river plume dynamics in southern Lake Michigan were analyzed using three-dimensional hydrodynamic and transport models. The relative importance of various physical and biological processes influencing the fate and transport of EC were examined via budget analysis and a first-order sensitivity analysis of model parameters. The along-shore advective flux of EC (CFU/m^2·s) was found to be higher compared to its cross-shore counterpart; however, the sum of diffusive and advective components was of a comparable magnitude in both directions showing the importance of cross-shore exchange in EC transport. Examination of individual terms in the EC mass balance equation showed that vertical turbulent mixing in the water column dominated the overall EC transport for the summer conditions simulated. Dilution due to advection and diffusion accounted for a large portion of the total EC budget in the nearshore, and the net EC loss rate within the water column (CFU/m^3·s) was an order of magnitude smaller compared to the horizontal and vertical transport rates. This result has important implications for modeling EC at recreational beaches; however, the assessment of the magnitude of EC loss rate is complicated due to the strong coupling between vertical exchange and depth-dependent EC loss processes such as sunlight inactivation and settling. Sensitivity analysis indicated that solar inactivation has the greatest impact on EC loss rates. Although these results are site-specific, they clearly bring out the relative importance of various processes involved.

1. Introduction

Increased beach closures due to impaired water quality have been a cause for concern in recent years. Numerous studies have shown a causal relationship between illnesses such as gastrointestinal disease and recreational-water quality as measured by indicator bacteria such as *Escherichia coli* (EC) and enterococci (*1*). Coastal water quality has a significant impact not only on human health but also on local economies (*2*). One study estimated economic losses as a result of closing a Lake Michigan beach due to pollution as ranging between $7,935 and $37,030 per day (*2*). The presence of fecal indicator bacteria (FIB) in nearshore waters is used to determine beach closures. Predictive modeling of FIB represents an attractive alternative to the traditional approach based on observation; however, to further refine mechanistic and statistical models, an assessment of the relative importance of different processes influencing FIB levels is needed. Significant progress has already been made in describing the concentration of indicator bacteria at marine and freshwater beaches using mathematical models (*3*−*8*). In addition, there is a large body of literature (mainly based on field and laboratory studies) on the importance of various mechanisms influencing FIB levels in coastal waters; however, the information is often qualitative in nature. To the best of our knowledge, a systematic budget analysis of FIB examining fluxes and the relative importance of various processes using field observations and detailed mechanistic modeling is not available in the literature. A notable exception is the work of Kim et al. (*3*) who applied a macroscopic mass budget analysis based on the Reynolds transport theorem to determine the sources of pollution for a marine beach in California. Budget analysis is important for identifying the key components of a predictive model and is a nontrivial task for a number of reasons. First, a majority of the beach sites in many states are impacted by unknown sources of contamination. An uncertainty in the nature, strength, and location of sources introduces significant uncertainty into the modeling making it difficult or impossible to infer processes. Second, a number of complex and often interrelated processes control the levels of FIB in nearshore waters including turbulent diffusion and dispersion, along-shore transport, growth, natural mortality, sunlight-dependent inactivation, sedimentation, and resuspension. Hipsey et al. (*9*) recently described these processes in detail within the context of process-based modeling. FIB levels in the water column are influenced by processes that are time-dependent and fully three-dimensional in nature placing significant demands on data and computational resources for 3D modeling (e.g., high-resolution bathymetry, time series of hydrodynamic and FIB data, etc.). Liu et al. (*8*) used two-dimensional, vertically integrated flow and transport models to describe the fate and transport of EC and enterococci at two beaches (Mt. Baldy and Central Avenue) along the Indiana shoreline in Southern Lake Michigan. Their modeling indicated that two nearby creeks draining into Lake Michigan are the primary sources of contamination impacting the beaches. Nevers and Whitman (*10*) recently examined EC data from 12 beaches along a 35-km length of the Indiana shoreline and proposed improved statistical models with only two variables: the wave height and an interaction term containing wind direction and creek turbidity. An assessment of the relative importance of different processes in the nearshore is needed for identifying the essential components of a predictive (either statistical or mechanistic) model. The aim of this paper is therefore to (a) combine fully three-dimensional hydrodynamic and transport modeling with observed concentrations of EC at the beach sites described in Liu et al. (*8*) to quantify various fluxes of EC (due to advection, diffusion, inactivation) as a function of time; (b) report the results of a sensitivity analysis of different

* Corresponding author e-mail: phani@msu.edu; phone: (517) 432-0851.
[†] Michigan State University.
[‡] University of Michigan.
[§] NOAA Great Lakes Environmental Research Laboratory.
[||] Lake Michigan Ecological Research Station.

10.1021/es902232a

Published on Web 12/31/2009

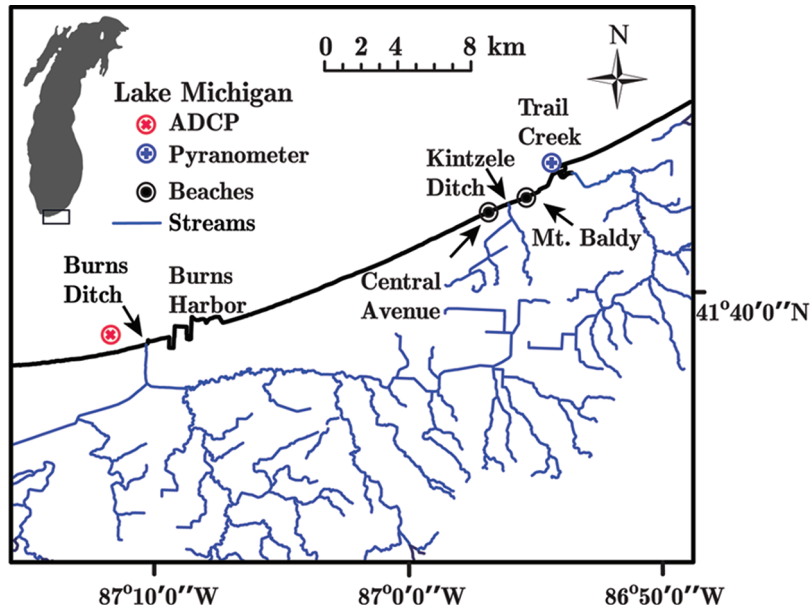

FIGURE 1. Map of Southern Lake Michigan and the Indiana Shoreline.

parameters influencing EC levels and rank them in order of importance; and (c) examine processes within the water column including vertical velocity profiles and loss of EC within the water column to understand the importance of the vertical dimension.

2. Materials and Methods

The primary area of interest includes approximately 72 km of Lake Michigan shoreline within the state of Indiana. Since summer is the primary swimming season and the lake freezes over in winter, hydrodynamic and water quality data were collected during the summer months at two beach sites (Mt. Baldy and Central Avenue, shown in Figure 1). Also shown in Figure 1 are the three main tributaries. Tributaries contributing flow to Lake Michigan within the study region are Burns Ditch (USGS 04095090) near Burns Harbor, Trail Creek at Michigan City Harbor (USGS 04095380), and Kintzele Ditch. Based on historical water quality monitoring data and the modeling study reported in Liu et al. (*8*), Kintzele Ditch and Trail Creek are considered to be the main sources of EC impacting the two beaches for the period of simulation (July−August 2004). Water samples were collected in knee-deep water at the two beaches during the summer months (July−August, 2004) when beach attendance is highest. Daily samples were also collected at nearby outfalls, Trail Creek and Kintzele Ditch, which represent sources of bacterial contamination for the beaches. A stage-discharge relation was established for the Kintzele Ditch site. Samples were collected and analyzed for EC using membrane filtration technique as described in ref *8*. Further details of these analyses as well as model inputs for the two tributaries (flow, temperature and EC time series) are available in ref *8*. Hydrodynamic data were collected during the summers of 2004 and 2006 near Burns Ditch using a 600 kHz Teledyne RD Instruments Acoustic Doppler Current Profiler (ADCP) deployed in an upward looking configuration. For the 2006 deployment data reported in this paper, the ADCP was located at a depth of 10.6 m at coordinates N 41° 38.120, W 87° 12.179. Examination of the 2004 ADCP data indicated potential issues with an internal compass, therefore the 2006 data were used to validate the hydrodynamic model used in the study. Solar radiation was measured at Trail Creek using a Campbell Scientific total radiation pyranometer. Locations of both instruments are shown in Figure 1.

3. Modeling

Since our primary interest was in examining EC fluxes in different coordinate directions, we used fully three-dimensional hydrodynamic and transport models to describe flow, temperature, and EC concentration fields as a function of space (x,y,z) and time t. The Princeton Ocean Model (POM), which uses a mode-splitting strategy to increase accuracy and reduce computational time, was used in the present study. POM solves the hydrodynamic primitive equations (details are available in the Supporting Information) and makes the Boussinesq and hydrostatic assumptions in the vertical so that density variations are neglected except in the computation of the buoyancy force. The horizontal plane was discretized using an Arakawa-C grid, and explicit time stepping using the leapfrog method was used. Details of the POM model are available in ref *11*. In the EC transport equation (details are available in Supporting Information), the loss rate k has the following form:

$$k = -\left(\frac{f_p v_S}{\Delta z_i} - \frac{f_p v_S}{\Delta z_{i-1}} + k_I I_0(t) e^{-k_e z} + k_d\right)\theta^{T-20} \qquad (1)$$

where the first two terms in the parentheses denote loss of EC due to settling to the layer below and gain from the layer above, and Δz_i, Δz_{i-1} denote the thicknesses of layers i, $i-1$. T denotes the temperature, f_P denotes the fraction of EC attached to particles, v_S is the settling velocity, k_I is the sunlight-dependent inactivation rate, $I_0(t)$ is the sun light at the surface, k_e denotes the extinction coefficient, and k_d is the base mortality rate (also called the dark death rate). The attenuation of sunlight within the water column was modeled using the Beer−Lambert relation. Dependence of the loss rate k on temperature was modeled using the Arrhenius relation as shown in eq 1. In addition to solving the equations of momentum, temperature, and EC concentration, the model uses the Mellor-Yamada 2.5 level turbulence parametrization and solves equations for turbulent kinetic energy and turbulence length scale. Nearshore circulation is influenced by the large-scale lake-wide circulation patterns. This effect was modeled by running the hydrodynamic model in a nested grid configuration. The whole-lake coarse grid model used a 2 km uniform grid spacing and 20 sigma layers in the vertical direction (*12*). The results were then used to drive the nearshore fine grid model, which used a 100 m uniform

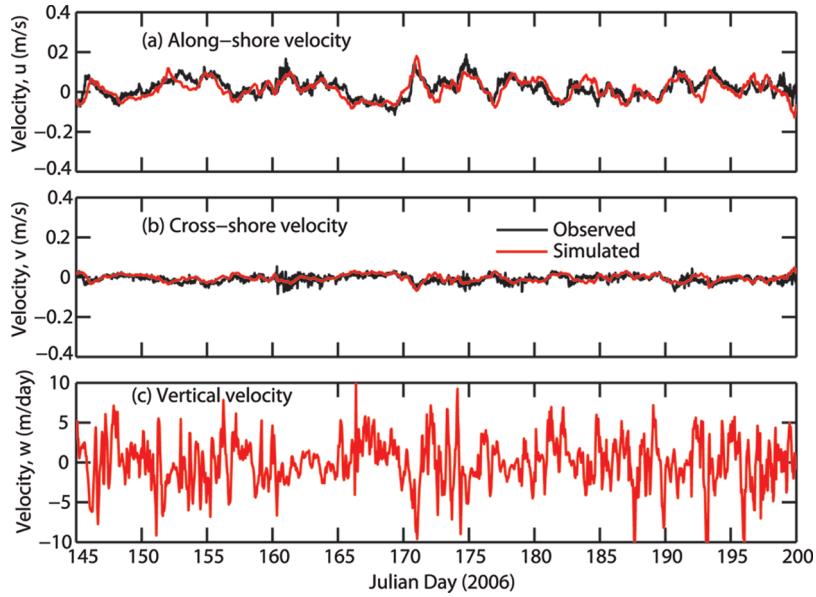

FIGURE 2. Comparison of (a) observed and simulated along-shore current (vertically integrated), (b) cross-shore current component (vertically integrated), and (c) simulated vertical velocity component *w* for the top layer (note the change in units: m/day).

grid and the same number of vertical levels as the coarse grid. Information transfer between the two models was one-way with results of the coarse grid model interpolated to the boundary of the fine grid. This method allowed us to simulate nearshore hydrodynamics accurately while avoiding the problem of specifying arbitrary open boundary conditions for the fine-scale model. The two computational domains as described by the coarse and fine grids are shown in the Supporting Information. The POM version used in the present study was adapted to the Great Lakes and was tested extensively in the past (*13*). Heat and momentum inputs to the surface of the lake were used as model forcing functions during simulation. Hourly meteorological data including cloud cover, air and dew point temperature, wind speed and direction were obtained for several stations from the NOAA National Climatic Data Center and NOAA National Data Buoy Center and interpolated to the model grid. Water level data were obtained from the Center for Operational Oceanographic Products and Services (CO-OPS), NOAA, and the National Data Buoy Center. Surface heat flux was calculated in the model to simulate temperature and the thermal structure in the lake using heat flux methods described in ref *14*. Briefly, the surface heat flux was calculated as the sum of short-wave radiation from the sun, sensible and latent heat transfer, and the long-wave back radiation to space. Due to the dependence of EC inactivation on the short-wave radiation, this component was of particular interest in this work. The short-wave radiation $I(t)$ was calculated based on its clear-sky value (calculated using the EPA method, (*15*)) and as a function of cloud cover. A comparison between the calculated and observed short-wave radiation was presented in the Supporting Information. The finite-difference numerical model was solved on a cluster computer at Michigan State University and was compiled and optimized for the parallel environment.

4. Results

The hydrodynamic model was tested by comparing simulations with current measurements made during the summer of 2006. Comparisons of the observed and simulated (vertically integrated) velocities (Figures 2a and b) show that currents in the nearshore are characterized by a strong along-shore (u) component and a relatively weak cross-shore (v) component. The dominant along-shore velocity component means that contaminant plumes tend to follow isobaths and nearshore−offshore advective exchange is limited by the small cross-shore current component. Frequent flow reversals observed during field studies (*16*) and reproduced in our simulations also increase dilution of contaminant plumes in the nearshore regions. Vertical velocities are relatively small and comparable in magnitude to the settling velocities used (5−10 m/day) in earlier studies (*5, 8*). Turbulent fluctuations in the vertical velocity (Figure 2c) could significantly increase the residence time of particles in the water column. Model comparisons with observed vertical velocity profiles are shown in Figure 3 to demonstrate the model's ability to reproduce vertical variations in velocity. Turbulent mixing and shear in the vertical produced well-mixed conditions; however, it is possible for vertical variations to be much more significant in the presence of stratification.

Exposure to sunlight, in particular the UV bandwidths, causes inactivation of bacteria due to direct DNA damage (*17, 18*) although photo-oxidative effects are the primary inactivation mechanism in surface waters due to the high attenuation of short UV wavelengths (*9*). Due to lack of detailed information on the attenuation characteristics of different wavelengths in the water column relative to the action spectrum of EC, shortwave radiation $I_0(t)$ considered in our modeling included all wavelengths between 150 and 3000 nm with a single attenuation coefficient k_e. Although the inactivation effect weakens at higher wavelengths, the justification for this choice is based on the fact that the higher wavelength energies excite sensitizer compounds that eventually oxidize organic molecules (*9*). Calculated shortwave radiation based on the geographic location, time of the year, time of the day, and the reported cloud cover is included in the Supporting Information. Effect of cloud cover on ambient sunlight was included in the model by interpolating observed values recorded at meteorological stations along Lake Michigan shoreline. Reasonable agreement was obtained between the observed and calculated solar radiation indicating that the radiation algorithms are suitable for making EC predictions except on days with significant cloud cover. Spatial and temporal variability of cloud cover and errors in interpolating this over large areas could be the reason for the model's inability to predict ambient sunlight on days with significant cloud cover.

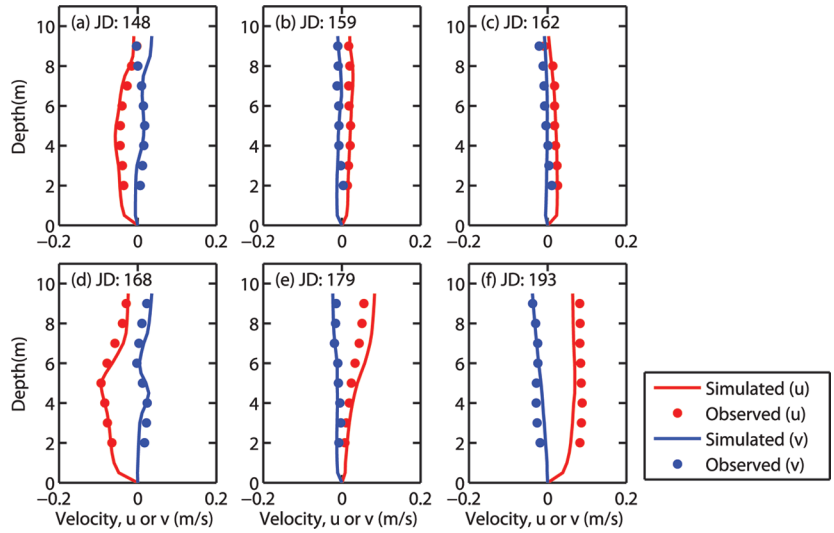

FIGURE 3. Comparison of observed and simulated vertical velocity profiles for along-shore (*u*) and cross-shore (*v*) velocities on different days during summer 2006.

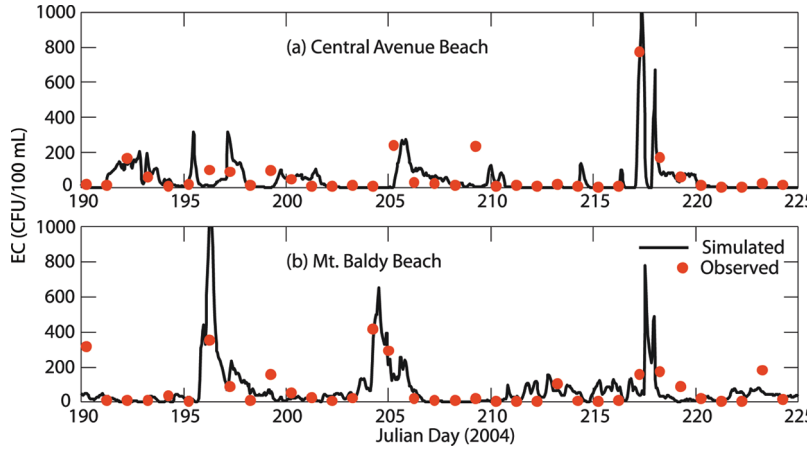

FIGURE 4. Observed and simulated EC concentrations at (a) Central Avenue Beach and (b) Mt. Baldy Beach.

Comparisons between observed and simulated EC for one set of parameters is shown in Figure 4. Reasonable agreement was obtained for the following set of parameters: a light-dependent inactivation rate (k_I) of 0.0026 W^{-1} m^2 d^{-1} (3×10^{-8} W^{-1} m^2 s^{-1}), a base mortality rate (k_d) of $8.6 \times 10^{-5} d^{-1}$ (10^{-9} s^{-1}), a settling velocity $v_S = 1$ m/d (based on the estimates in *19*) with an attached EC fraction $f_P = 0.1$ (*5*) and a light extinction coefficient of 0.55 m^{-1}. It is important to note that the formulation used (eq 1) to describe EC losses does not allow us to uniquely estimate model parameters since any combination of parameters that produces the same *net* loss of EC (relative to a conservative tracer) will still result in a good agreement with data. Although our model describes the attenuation of incident sunlight (and hence inactivation) with depth, k_I itself is the result of more complex processes (*9*). To estimate k_I uniquely, fundamental processes such as dynamic attachment to particles, suspended sediment transport including settling and resuspension, attenuation of different bandwidths of incident radiation within the water column as a function of suspended material, dissolved oxygen, etc. need to be simulated; however, this will further complicate the modeling in addition to introducing several new model parameters. As noted earlier, the net loss of EC relative to the hydrodynamic processes of advection and diffusion can be quantified uniquely using our modeling. Observed and simulated concentrations presented as probability plots in the Supporting Information indicate that the high as well as low levels of EC can be described using the current model. Modeling results (and rates) presented here are similar to those shown in Liu et al. (*8*) although the present model described the data better. For example, the RMSE value based on log-transformed EC concentrations for the Mt. Baldy beach is 0.41 for the present 3D model compared to a value of 0.808 reported in Liu et al. (*8*) for a vertically integrated model. The improvement in RMSE is partly due to the use of 3D models and partly due to refinements in input—3 arc-second bathymetry blended with high-resolution LIDAR data was used in our nearshore modeling. The inactivation formulation (eq 1) in this paper used a base mortality rate which was absent in *8*. To quantify the relative importance of various processes contributing to the loss of EC, we conducted a first-order sensitivity analysis and computed condition numbers for each parameter. The condition number for a parameter k (defined as $C_k = (k/c)(\partial c/\partial k)$ where c denotes EC concentration) is higher for parameters that produce large variations in model predictions. Computed condition numbers for parameters k_I, f_P, v_S, k_d, and k_e are 83, 58, 99, 63, and 102, respectively, indicating that the extinction coefficient for sunlight in the water column is the most important parameter in eq 1. Examination of the relative contributions of various EC loss mechanisms indicated that for the parameters used in Figure 4, sunlight inactivation accounted for 96% of the total losses in the water column, while base mortality and settling accounted for the remaining 4% of the losses.

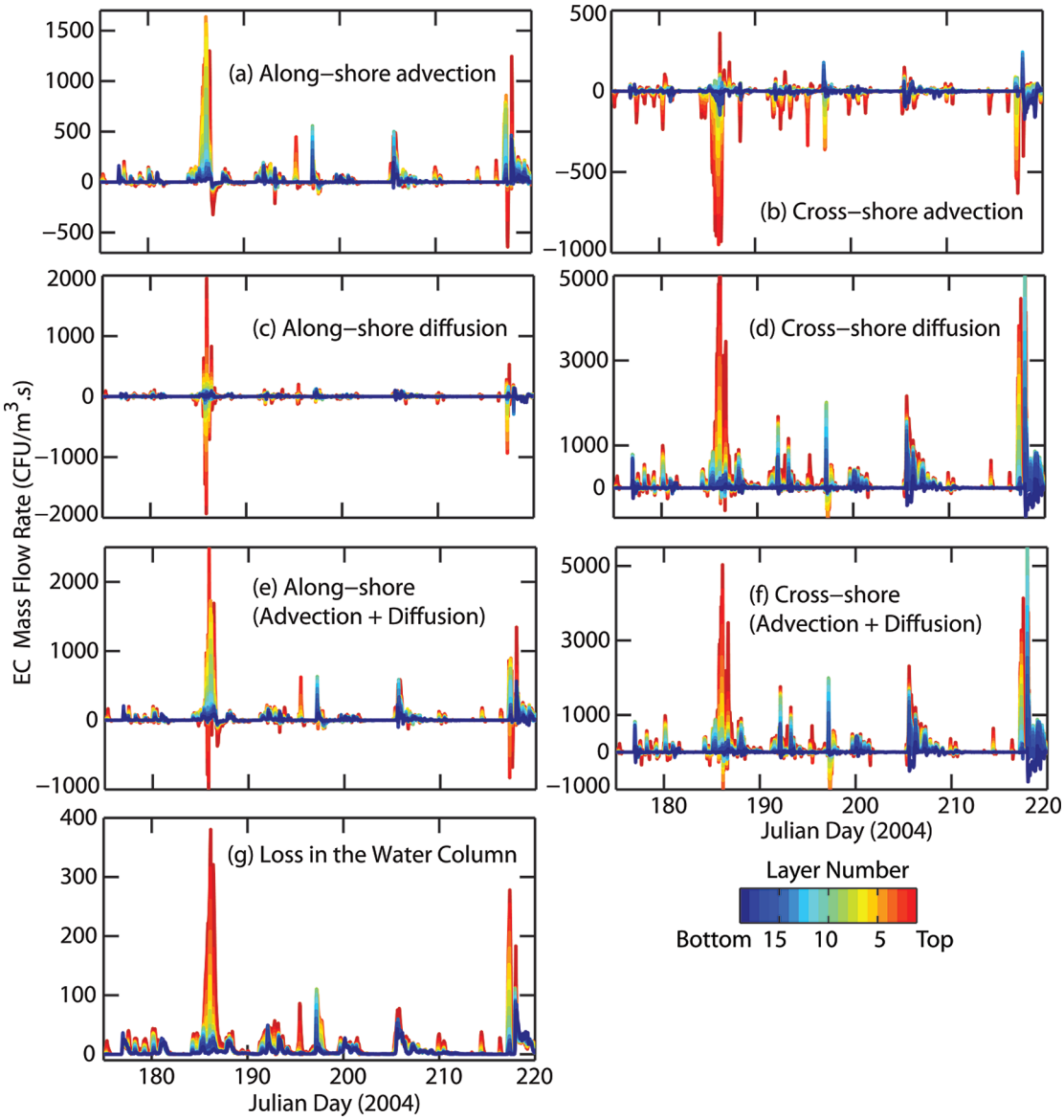

FIGURE 5. Results of budget analysis for EC showing the relative contributions of different processes within the water column. Each term in the 3D transport equation, which represents a mass flow rate for EC, is plotted for all layers in the figures. (a) and (b) The horizontal advective terms in the along-shore and cross-shore directions respectively: $\partial(uc)/\partial x$, $\partial(vc)/\partial y$. (c) and (d) The horizontal diffusive terms $\partial/\partial x(-A_H\ \partial c/\partial x)$, $\partial/\partial y(-A_H\ \partial c/\partial y)$ in the along-shore and cross-shore directions respectively. Here A_H denotes the horizontal eddy diffusivity for EC. (e) and (f) Sum of the advective and diffusive terms in the along-shore and cross-shore directions respectively. (g) Total EC loss in the water column due to settling, solar inactivation and base mortality (temperature effect is included).

Periods of high bottom-shear stress, caused by currents or wind-generated waves, can cause bacteria within the top layers of the sediment to resuspend into the water column along with sediment. Although a detailed analysis of the role of sediment is not the focus of this paper, results presented in the Supporting Information provide an indication of the importance of sediment as a possible source of contamination. Comparisons between normalized values of the total bottom shear stress and observed EC ($p - p_{min}/p_{max} - p_{min}$, where p denotes EC concentration or the shear stress) show that while sediment resuspension is a complex nonlinear process with significant spatial variability, some of the peaks in EC could be due to sediment resuspension. Perhaps more important is the observation that at the study site the sediment appears to represent a time-dependent source of finite size so that a single high shear stress event has the potential to resuspend virtually all the EC on the sediment bed leaving subsequent shear events with no more EC to resuspend until further deposition takes place. This behavior, which can be seen around Julian days 220 and 225, has important implications for modeling EC deposition and resuspension.

Contaminant transport in southern Lake Michigan is characterized by the presence of a dominant along-shore velocity component and a relatively weak cross-shore component. Frequent reversals in direction of the along-shore velocity are also observed (*16*). Sharp fronts are sometimes observed increasing the importance of nearshore−offshore exchange due to large cross-isobath gradients (*20*). To better understand the relative importance of these processes and to quantify EC fluxes in the nearshore, we conducted a budget analysis by examining the fluxes entering and leaving a control volume (100 m long in the along-shore direction, 100 m wide in the cross-shore direction, and 4.5 m deep at the center) at the Central Avenue beach. EC fluxes due to advection and turbulent

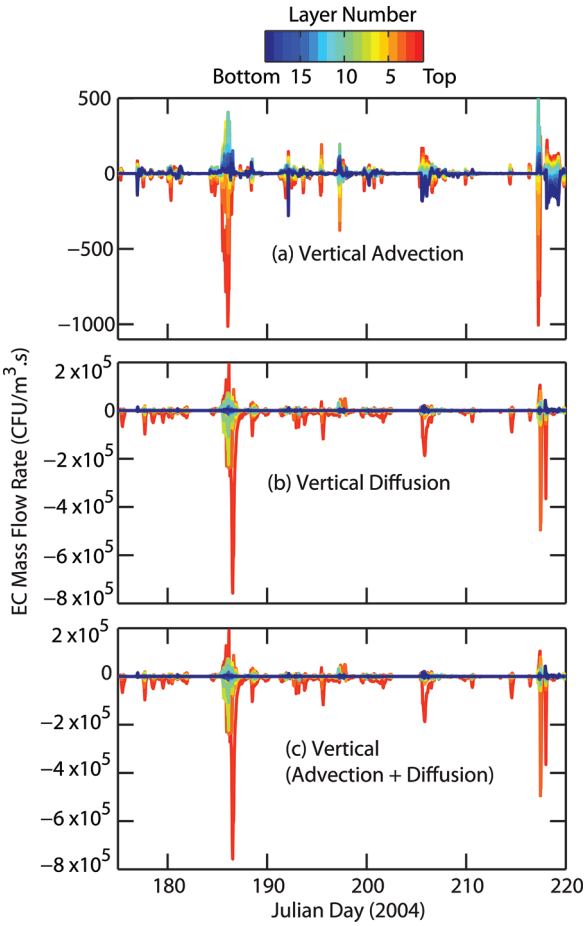

FIGURE 6. Variation of the magnitudes of vertical advection and diffusion within the water column as a function of time. Terms in the 3D transport equation in the *z*-direction, which represent a mass flow rate for EC, are plotted for all layers in the figures. (a) vertical advective term, $\partial(wc)/\partial z$; (b) vertical diffusive term, $\partial/\partial z(-K_V \partial c/\partial z)$; (c) the sum of vertical advective and diffusive terms.

diffusion, as well as the net flux as defined below were calculated in different directions.

$$J_{\text{adv,x}} = uc, J_{\text{adv,y}} = vc, J_{\text{adv,z}} = wc$$
$$J_{\text{diff,x}} = -A_H \frac{\partial c}{\partial x}, J_{\text{diff,y}} = -A_H \frac{\partial c}{\partial y}, J_{\text{diff,z}} = -K_V \frac{\partial c}{\partial z} \quad (2)$$

Here u, v, w denote the velocity components in the along-shore (x), cross-shore (y), and vertical (z) directions, and A_H, K_V denote the eddy diffusivity for EC in the horizontal and vertical directions, respectively. Temporal variation of the fluxes (defined in eq 2) within the control volume is included in the Supporting Information. Examination of the fluxes in eq 2 indicated that advective transport in the along-shore direction dominated over its cross-shore counterpart; however, the sum of advective and diffusive fluxes was comparable in the two directions. Smaller cross-shore velocity component resulted in greater concentration gradients in the offshore direction so that nearshore−offshore exchange was dominated by diffusion processes. Dilution due to advection and diffusion accounted for a significantly large portion of the total EC flux in the nearshore. While information about the fluxes is useful, it does not provide information about the relative importance of different processes. To understand this, the individual terms representing advection, diffusion, and loss processes in the EC transport equation (with units CFU/m^3·s) were computed and are plotted in Figures 5 and 6. It is clear that net mass flow rate in the along-shore direction was comparable to that in the cross-shore direction. However, while the advective along-shore component of the mass flow rate was almost always positive (inflow into the control volume is positive, Figure 5), the advective component in the cross-shore direction was usually negative and caused removal of contamination from the cell. Net mass flow rate, however, was almost always positive in both along-shore and cross-shore directions indicating that contaminant plume behavior is complex in the presence of frequent flow reversals (*16*) and constantly varying concentration gradients. Figure 6 reveals that vertical transport in the water column was dominated by turbulent mixing, and transport rates in the upper layers were significantly greater than those in the lower layers (Figures 5 and 6) resulting in a complicated 3D plume front, which cannot be adequately described using vertically integrated models. The high vertical diffusion (Figure 6b) indicates well-mixed conditions due to turbulence in the water column. We also notice that the total loss term (due to settling, light, and base mortality) was an order of magnitude smaller compared to the horizontal advection terms. This result has two important implications. First, for well-mixed summer conditions similar to those simulated here, EC plume shapes can be predicted well using models similar to the present one if sources and loading are known. Second, for highly stratified flows depth-dependent EC loss mechanisms (such as sunlight-dependent inactivation) could assume much greater importance in describing EC concentrations in the vertical compared to the conditions simulated here. The tight coupling between vertical transport and inactivation leads us to conclude that simulation of more fundamental processes (e.g., suspended sediment transport, attenuation of different light energies within the water column, etc.) is required to quantify the loss of EC in the water column for well-mixed and stratified cases alike since conditions in the water column are dynamic. Although these results are site-specific and cannot be generalized to all beaches, they have important implications for modeling beaches impacted by river plume dynamics in the Great Lakes region.

5. Discussion

In this paper we examined the relative importance of processes influencing the fate and transport of FIB in the nearshore region of Lake Michigan and demonstrated the complex nature of the processes involved. ADCP measurements of currents were used to validate the hydrodynamic model. EC observations at sources and nearby beaches have been used to show that biological processes can be modeled accurately for summer conditions using the present model. For the conditions simulated here, dilution due to advection and diffusion was an order of magnitude higher compared to the net loss processes within the water column. Budget analysis considering individual terms in the EC mass balance equation indicated that turbulent mixing within the water column dominated the overall EC transport consistent with our observations of well-mixed conditions at the site (e.g., uniform vertical profiles of velocity and temperature). The amount of vertical mixing in the water column is controlled by the degree of density stratification in the nearshore, therefore simulation results depend, among other factors, on inflows (volume of water entering the lake per unit time) as well as source conditions including water temperature and the vertical distribution of materials at the source. Thermal buoyancy contribution of inflowing water as well as conditions at the source (well-mixed based on our observations) were taken into account in our modeling. Strong vertical stratification can prevent vertical mixing changing the importance of processes in the water column. The importance of vertical mixing is site-specific (and changes with time at a given site), but useful insights can be obtained

by comparing EC plume dynamics at different sites based on dimensionless numbers such as the gradient Richardson number (which represents the opposing contributions of buoyancy and shear). A more accurate estimation of the importance of various EC loss processes will require refinements to the inactivation formulation used in this work. For example the effect of water clarity (CDOM and SSC) on inactivation rates can be quantified by coupling EC and sediment transport models to better understand the linkages between environmental variables and EC levels. High-frequency biological observations are also needed to accurately assess the importance of biological processes associated with different time scales. Analysis of the bottom shear stresses due to current and waves in the nearshore reveals a connection between observed EC peaks and high shear stress events. Linkages between these processes can be studied by coupling sediment transport descriptions with a wind-driven current and wave model. Results of sensitivity analysis clearly demonstrate the importance of sunlight inactivation and the role played by the extinction coefficient associated with different wavelength bands. Quantitative information on the attenuation of different energy bands within the water column and their role in EC inactivation is needed to further refine EC fate and transport models.

Acknowledgments

This research was funded by the NOAA Center of Excellence for Great Lakes and Human Health. Computer time on the cluster computer at the MSU High Performance Computing Center (HPCC) is gratefully acknowledged. This article is Contribution 1562 of the USGS Great Lakes Science Center.

Supporting Information Available

Additional comparisons as well as details of the model, budget analysis, and numerical methods used. This material is available free of charge via the Internet at http://pubs.acs.org.

Literature Cited

(1) Prüss, A. A review of epidemiological studies from exposure to recreational water. *Int. J. Epidemiol.* **1998**, *27*, 1–9.
(2) Rabinovici, S. J. M.; Bernknopf, R. L.; Wein, A. M.; Coursey, D. L.; Whitman, R. L. Economic and health risk trade-offs of swim closures at a Lake Michigan beach. *Environ. Sci. Technol.* **2004**, *38* (10), 2737–2745.
(3) Kim, J. H.; Grant, S. B.; McGee, C. D.; Sanders, B. F.; Largier, J. L. Locating sources of surf zone pollution: A mass budget analysis of fecal indicator bacteria at Huntington Beach, California. *Environ. Sci. Technol.* **2004**, *38* (9), 2626–2636.
(4) Sanders, B. F.; Arega, F.; Sutula, M. Modeling the dry-weather tidal cycling of fecal indicator bacteria in surface waters of an intertidal wetland. *Water Res.* **2005**, *39* (14), 3394–3408.
(5) McCorquodale, J. A.; Georgiou, I.; Carnelos, S.; Englande, A. J. Modeling coliforms in storm water plumes. *J. Environ. Eng. Sci.* **2004**, *3* (5), 419–431.
(6) Grant, S. B.; Kim, J. H.; Jones, B. H.; Jenkins, S. A.; Wasyl, J.; Cudaback, C. Surf zone entrainment, along-shore transport, and human health implications of pollution from tidal outlets. *J. Geophys. Res.-Oceans* **2005**, *110* (C10), 20.
(7) Boehm, A. B.; Keymer, D. P.; Shellenbarger, G. G. An analytical model of enterococci inactivation, grazing, and transport in the surf zone of a marine beach. *Water Res.* **2005**, *39* (15), 3565–3578.
(8) Liu, L.; Phanikumar, M. S.; Molloy, S. L.; Whitman, R. L.; Shively, D. A.; Nevers, M. B.; Schwab, D. J.; Rose, J. B. Modeling the transport and inactivation of *E. coli* and enterococci in the near-shore region of Lake Michigan. *Environ. Sci. Technol.* **2006**, *40* (16), 5022–5028.
(9) Hipsey, M. R.; Antenucci, J. P.; Brookes, J. D. A generic, process-based model of microbial pollution in aquatic systems. *Water Resour. Res.* **2008**, *44*, 7.
(10) Nevers, M. B.; Whitman, R. L. Coastal strategies to predict *Escherichia coli* concentrations for beaches along a 35 km stretch of southern Lake Michigan. *Environ. Sci. Technol.* **2008**, *42* (12), 4454–4460.
(11) Mellor, G. L. *Users Guide for A Three-Dimensional, Primitive Equation, Numerical Ocean Model*; Princeton University: Princeton, NJ, 2004; p 56.
(12) Beletsky, D.; Schwab, D. J. Climatological circulation in Lake Michigan. *Geophys. Res. Lett.* **2008**, *35*, L21604; 10.1029/2008GL035773.
(13) Beletsky, D.; Schwab, D. J. Modeling circulation and thermal structure in Lake Michigan: Annual cycle and interannual variability. *J. Geophys. Res.-Oceans* **2001**, *106* (C9), 19745–19771.
(14) McCormick, M. J.; Meadows, G. A. An intercomparison of four mixed layer models in a shallow inland sea. *J. Geophys. Res.-Oceans* **1988**, *93* (C6), 6774–6788.
(15) *Effect of Geographical Location on Cooling Pond Requirements and Performance*; Report 16130FDQ; U.S. Environmental Protection Agency: Washington, DC, 1971; p 160.
(16) Nevers, M. B.; Whitman, R. L.; Frick, W. E.; Ge, Z. Interaction and influence of two creeks on *Escherichia coli* concentrations of nearby beaches: Exploration of predictability and mechanisms. *J. Environ. Qual.* **2007**, *36*, 1338–1345.
(17) Whitman, R. L.; Nevers, M. B.; Korinek, G. C.; Byappanahalli, M. N. Solar and temporal effects on *Escherichia coli* concentration at a lake Michigan swimming beach. *Appl. Environ. Microbiol.* **2004**, *70* (7), 4276–4285.
(18) Sinton, L. W.; Hall, C. H.; Lynch, P. A.; Davies-Colley, R. J. Sunlight inactivation of fecal indicator bacteria and bacteriophages from waste stabilization pond effluent in fresh and saline waters. *Appl. Environ. Microbiol.* **2002**, *68* (3), 1122–1131.
(19) Eadie, B. J. In *Probing Particle Processes in Lake Michigan Using Sediment Traps*, 1997; pp 133−139.
(20) Rao, Y. R.; Schwab, D. J. Transport and mixing between the coastal and offshore waters in the great lakes: a review. *J. Great Lakes Res.* **2007**, *33* (1), 202–218.

ES902232A